Solidis Status Management of the Status of t

reprint





Amorphous silicon solar cells on nano-imprinted commodity paper without sacrificing efficiency

C. H. M. van der Werf^{*}, T. Budel, M. S. Dorenkamper, D. Zhang, W. Soppe, H. de Neve, and R. E. I. Schropp^{**}

Solliance-ECN, High Tech Campus 21, 5656 AE Eindhoven, The Netherlands

Received 21 August 2015, revised 12 October 2015, accepted 13 October 2015 Published online 20 October 2015

Keywords photovoltaics, paper, hot wire chemical vapour deposition, solar cells, amorphous materials, silicon

Paper is a cheap substrate which is in principle compatible with the process temperature applied in the plasma enhanced chemical vapour deposition (PECVD) and hot wire CVD (HWCVD) of thin film silicon solar cells. The main drawback of paper for this application is the porosity due to its fibre like structure. The feature size (micrometre scale) is larger than the thickness of the applied photovoltaic layers. To overcome this problem, UV curable lacquer was used to planarize the surface. Plain 80 grams printer paper was taken as a substrate and the lacquer smoothens the rough surface of the paper

such that a designed nanostructure can be imprinted for light scattering. In this manner single junction amorphous silicon solar cells with a HWCVD deposited intrinsic layer were processed on paper, without any concessions to the process temperature of 200 °C. The cell performance is comparable to that of reference cells grown on stainless steel, proving that solar cells can be deposited on paper substrates without sacrificing performance. PV on paper could be applied as "disposable" power source for gadgets, electronic labelling, remote sensing systems, etc. (Internet of Things).

© 2015 WILEY-VCH Verlag GmbH & Co. KGaA, Weinheim

1 Introduction Paper is a cheap substrate which is – in vacuum – in principle compatible with the process temperature (200 °C−300 °C) during PECVD and HWCVD deposition of thin film silicon solar cells. The main drawback of paper is its porosity due to its fibre like structure. If this can be overcome by planarizing the surface it would become possible to use paper or even fabric as a substrate for direct deposition of thin film silicon solar cells. Roll-toroll or sheet-to-sheet handling of paper is a widely spread technology. Together with the low costs of paper compared to glass, stainless steel or temperature compatible plastics the production costs of thin film silicon cells could be reduced significantly [1].

To keep the size of a production machine within a realistic and economically favourable range the deposition time of the consecutive layers should be as short as possible. Deposition of device quality hydrogenated nano-crystalline silicon (nc-Si:H) as an absorber layer in solar cells takes rather long (>30 min). With hydrogenated amorphous silicon (a-Si:H) it is possible to reach deposition rates for de-

vice quality material that allow the absorber layer to be deposited within 5 minutes, especially if HWCVD [2] is used rather than radio-frequent (RF) PECVD.

It is not likely that a-Si:H modules on paper will ever be used for large scale outdoor power production. The power production per m² of a-Si:H cells is too low to become economically feasible and due to the poor encapsulation properties of paper the costs for proper encapsulation of modules on paper will not be reduced.

However, for other applications of PV such as "disposable" power sources for gadgets, smart parcels, electronic labelling (Internet of Things), remote sensing systems, etc., 'paper solar cells' are very well feasible. For these applications the requirements for power and lifetime are far less stringent than for outdoor power production panels. Using cheap encapsulants the production costs can be low enough to use these cells in an economically feasible way to compete with batteries as power supplies for low-power applications such as product tracking, secure identification, and copy protection.

^{*} Corresponding author: e-mail vanderwerf@ecn.nl

^{**} Present address: Eindhoven University of Technology (TU/e), Department of Applied Physics, Plasma and Materials Processing, P.O. Box 513, 5600 MB Eindhoven, The Netherlands.

Recent research on solar cells on paper substrates predominantly dealt with organic semiconductor materials [3–5]. Recently Aguas et al. [6] showed that printing paper that contains a cast-coated layer of a hydrophilic mesoporous material can be used as a substrate for a 3.4% efficient thin film silicon solar cell, deposited at a temperature of 150 °C. In this paper we show the achievement of an efficiency that is almost twice as high (6.7%), using commodity printer paper as commonly used in office printers and copiers. This efficiency is reached using an UV curable acrylate lacquer that planarizes the paper and at the same time is nano-imprinted to provide a designed light absorption enhancement scheme. Due to the present work the performance on paper is now equal to that of state-of-the-art reference cells on a stainless steel substrate.

2 Experimental As substrates plain white copying paper (80 g/m²) used in office copying machines, and 100 µm thick stainless steel foil were used. The latter is used in our base-line nip (PECVD) a-Si:H process [7]. These stainless steel substrates were planarized by applying an UV curable acrylate lacquer (MO18, developed on customer specifications by C-coatings for the use in vacuum at 200 °C). The lacquer was imprinted with a periodic nano-texture (pitch and height of the master are 1 µm and 350 nm, respectively). After the imprinting the lacquer was cured by UV light. The process of planarization and nanoimprinting on stainless steel foil is described in more detail by Soppe et al. [8]. The paper was first impregnated with the same lacquer as used for the imprinting by doctor blade (set to 50 µm). After 10 minutes, to allow the lacquer to be uniformly soaked by the paper, the substrate was exposed for 5 minutes to UV-A light. Then a second lacquer layer was applied by doctor blade (set to 100 µm). This layer was imprinted and exposed for 5 minutes with UV-A light through the PDMS stamp. After removal of the stamp the lacquer was fully cured by a different, more intense UV (ABC) source. The impregnation and imprinting process took place at room temperature in air ambient. After curing, the substrates were cut to size $(10 \times 10 \text{ cm}^2)$, ultrasonically cleaned in 2-propanol, blow dried with N₂ and annealed at 200 °C during 2 hours in N₂ ambient. The annealing step of 2 hours at 200 °C (the deposition temperature of the a-Si:H) is sufficient to reduce the degassing rate of the lacquer from $1.4\times 10^{-6}\,\text{mbar}\cdot \text{l/s/cm}^2$ to $4\times 10^{-8}\,\text{mbar}\cdot \text{l/s/cm}^2$. Degassing rate and composition were determined by Philips Innovation Services using gas chromatography mass spectrometry on a 20 µm thick lacquer layer on glass. The main degassing products are phthalic anhydride and 2-oxepanone, which at the final low degassing rates during processing do not appear to significantly reduce the quality of a-Si:H. Subsequently a back reflector consisting of 300 nm Ag and 100 nm Al doped ZnO (ZnO:Al) was sputtered by means of RF magnetron sputtering in an AJA 2200 sputter tool. On top of that an a-Si:H nip layer stack (27 nm n-layer, 6 nm intrinsic buffer, 350 nm i-layer, 2 nm intrinsic buffer, 21 nm

p-layer) was deposited in a cluster tool (Pasta [9]) with both PECVD and HWCVD reactors. The doped and buffer layers were deposited by means of RF PECVD, the intrinsic layer by HWCVD (Ta filaments, 1800 °C). The highest substrate temperature used in this process was about 200 °C. The cells were finished by RF magnetron sputtering of 80 nm thick $4 \times 4 \text{ mm}^2$ Sn-doped In_2O_3 (ITO) squares through a shadow mask on top of which a gold grid was evaporated. As a final step the cells received an annealing treatment (2 hours, 140 °C, N_2 ambient).

The morphology of the substrate surface was characterized by SEM (JSM-6010LA IntouchScope) and AFM (Park NX10). The finished cells were characterized by JV measurements under AM1.5 conditions with a dual-source Wacom solar simulator and external collection efficiency (ECE) measurements with an Optosolar 300 setup.

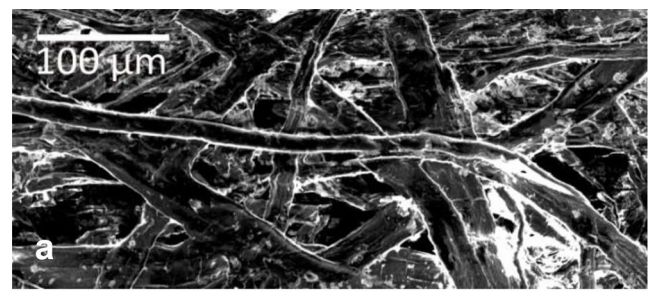
3 Results and discussion

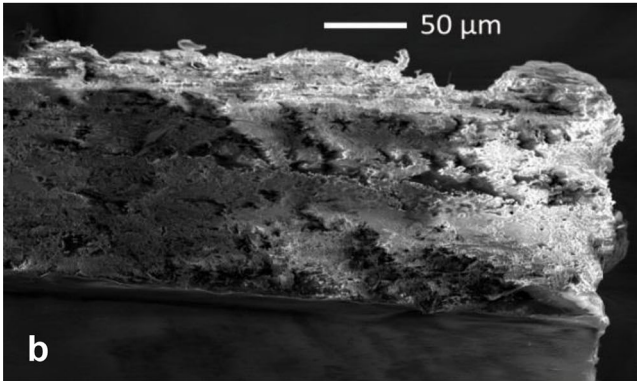
3.1 SEM and AFM on nano-imprinted back reflectors Figure 1(a) shows a SEM micrograph of the "surface" of untreated paper. It is clear that the roughness, or rather the porosity, of the paper is in the order of tens of micrometres which is two orders larger than the thickness of a-Si:H thin film solar cells (<500 nm). Although not shown here, for the stainless steel the surface feature size is still in the order of micrometres, i.e. larger than the thickness of the applied photovoltaic layers. Due to this roughness it is very unlikely that working solar cells can be produced directly on these substrates, especially on the paper.

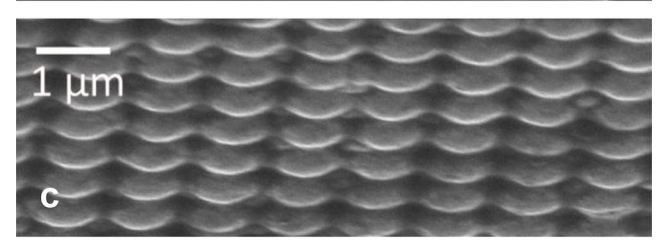
Therefore the surfaces of the substrates were transformed into more smooth and closed surfaces by applying an UV-curable acrylate lacquer which was nano-imprinted after application. Figure 1(b) shows a tilted (30°) SEM micrograph of the edge of an impregnated and imprinted paper substrate on the imprinted side coated with the Ag/ZnO: Al back reflector (visible in the bottom part of the micrograph). In Fig. 1(c) a close up of the surface of a completed cell is represented. A smooth nano-patterned surface is visible (confirmed by AFM as shown in Fig. 1(d)) showing that the lacquer can completely overcome the problem of the porosity and roughness of the substrates. Proof of the periodic texture can also be found in the colourful reflections from the areas outside of the completed cell contact pads visible in Fig. 1(e).

Besides the planarization of the substrate the nano-imprinted lacquer is used to enhance the optical performance of the solar cells deposited on these substrates. For the cells reported in this paper we replicated the morphology of a master which has a periodic structure with a pitch of 1 µm and a peak-to-valley roughness of around 350 nm. The effectiveness of this morphology, which was optimized for use in a-Si:H/nc-Si:H tandem solar cells, with regards to improved current generation was shown in earlier work [8]. Although this texture is not necessarily the optimum morphology for single junction a-Si:H cells we used it to demonstrate the possibility of nanopatterning simultaneously with eliminating the porosity of the paper









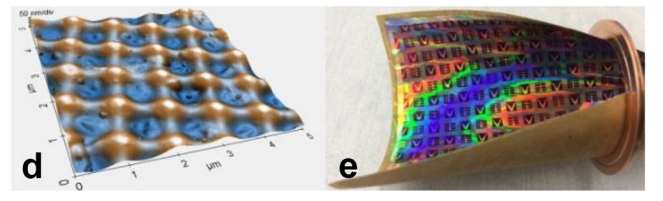
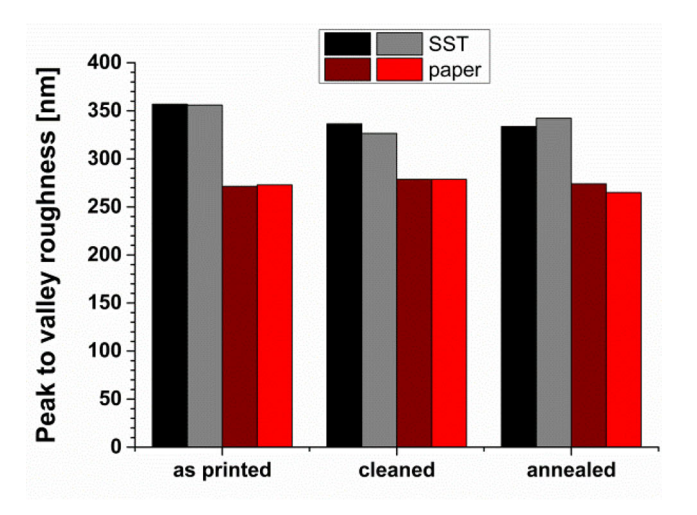


Figure 1 SEM micrographs of (a) untreated paper (top view), (b) impregnated and imprinted paper with metal/ZnO: Al back reflector (30° tilt angle), (c) surface of completed cell on paper (30° tilt angle), (d) isotropic 3D representation of the surface of impregnated and nano-imprinted paper obtained by AFM and (e) photograph of the completed cells $(10 \times 10 \text{ cm}^2)$ rolled up in a (CF-40) copper gasket.

as a substrate. Optimization of the design of the texture for specific cell types (absorber material, single junction or multi-junction) can be subject of future work.

During the transfer of this morphology to the lacquer and the subsequent curing, cleaning and annealing steps the original morphology of the master can change. To investigate the influence of the different substrates and the subsequent processing steps on the morphology the surface was scanned over an area of $5 \times 5 \ \mu m^2$ by AFM in noncontact mode. This was done for both the paper and the stainless steel substrate after curing of the imprinted lacquer, after ultrasonic cleaning and after annealing.



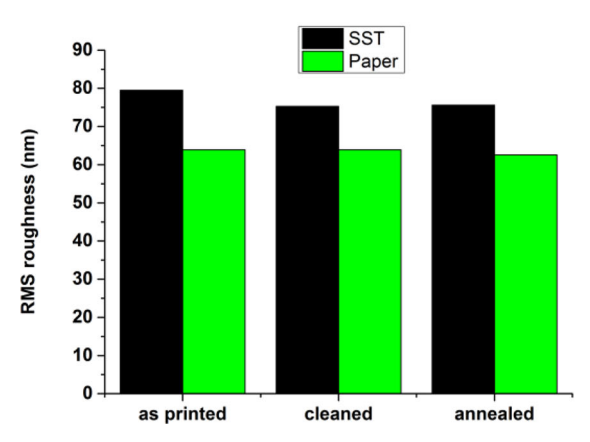


Figure 2 Peak-to-valley roughness (top) and root mean square (RMS) roughness (bottom) obtained from AFM scans on the nano-imprinted paper and stainless steel (SST) after curing (as printed), after cleaning and after annealing.

Figure 1(d) shows the result of one of these scans in an isotropic 3D representation for the cured lacquer on paper. It can be clearly seen that the surface has a periodic structure with a pitch of 1 µm. AFM scanning of both the paper and the stainless steel substrates after the subsequent process steps reveals that the pitch of the patterning does not change. However, the peak-to-valley roughness (R_{PV}) and the root mean square (RMS) roughness do change. Per scan R_{PV} was determined over two lines over the maxima diagonally across the scanned area perpendicular to each other. The RMS roughness was determined over the whole scan area of $5 \times 5 \mu m^2$. The thus obtained values are plotted in Fig. 2. From this it can be clearly seen that the roughness after curing on the paper substrate is substantially lower than on the stainless steel substrate (R_{PV} 272 nm vs. 356 nm, RMS roughness 64 nm vs. 80 nm). Cleaning and annealing does not have a significant influence on the roughness on the paper substrate. On the stainless steel substrate a small decrease in roughness is seen after cleaning. The paper does show discolouration during the annealing step from white to yellowish, showing

625

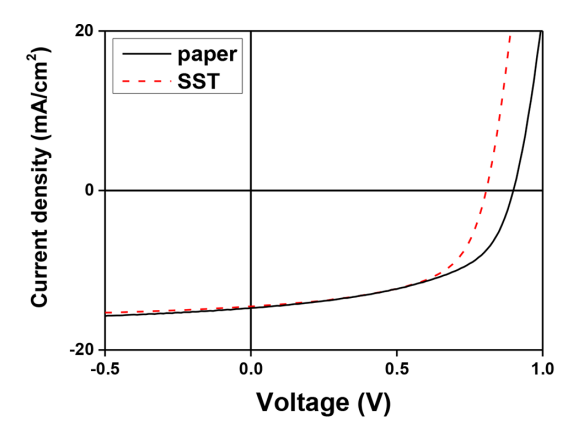
that the integrity of the cellulose fibres is affected. In spite of this, the annealing does not seem to have any further influence on the surface morphology, showing that shrinkage of the lacquer upon annealing does not play a major role and the integrity of the substrate as a whole is maintained.

As mentioned in Section 2, the paper is impregnated with lacquer. This lacquer may not completely fill all the pores in the paper and is not completely cured before the to-be-imprinted lacquer layer is applied. This leads to a soft underground for the imprint. Due to this softness it is likely that during the imprinting the paper/lacquer substrate is deformed. If then the stamp is removed this deformation is released, which explains a lower roughness compared to the imprint on the steel substrate.

3.2 Solar cell performance In Table 1 the average J-V parameters of the 10 best performing solar cells on each substrate are listed. In Fig. 3 (top) the J-V curves of the best performing cells on each substrate (paper and SST) are shown. The performance with respect to the efficiency (η) and short-circuit current (J_{SC}) is comparable for the two types of substrates. A significant difference can be found in the open-circuit voltage $(V_{\rm OC})$. On paper the $V_{\rm OC}$ is about 90 mV higher than on stainless steel. This might partially be due to the lower roughness of the back reflector on paper. The (RMS) surface roughness itself is not decisive for the value of the $V_{\rm OC}$. Properties like steepness, narrowness, and depth of the valleys in the morphology have significant influence on the $V_{\rm OC}$ [10–12]. As the pitch of the nanostructure remains the same (1 µm) but the height or depth is smaller on paper the structures are less steep or narrow resulting in a higher $V_{\rm OC}$. Furthermore, we speculate that the effective substrate temperature of the paper is somewhat lower during deposition than the stainless steel, due to its different radiative (higher emissivity) and lower heat conducting properties. The actual substrate temperature during deposition could not experimentally be determined. A lower substrate temperature is known to lead to higher bandgap material and thus higher $V_{\rm OC}$. Figure 3 (bottom) shows the external collection efficiency (ECE) measured with neither bias light nor bias voltage for the same cells depicted in Fig. 3a. The main difference is visible between 350 nm and 550 nm where the cell on paper performs somewhat better than the cell on stainless steel. This difference seems to be caused by a difference in

Table 1 Average of the J-V parameters of the ten best cells on the paper and the stainless steel (SST) substrate.

parameter	paper	SST	unit
$\overline{V_{ m OC}}$	897	811	mV
$V_{ m OC} \ J_{ m SC}$	13.9	13.8	mA/cm ²
FF	0.533	0.582	
η	6.7	6.5	%
$R_{ m s}$	7.4	6.6	$\Omega \ { m cm}^2$
$R_{\rm p}$	368	482	$\Omega \ { m cm}^2$



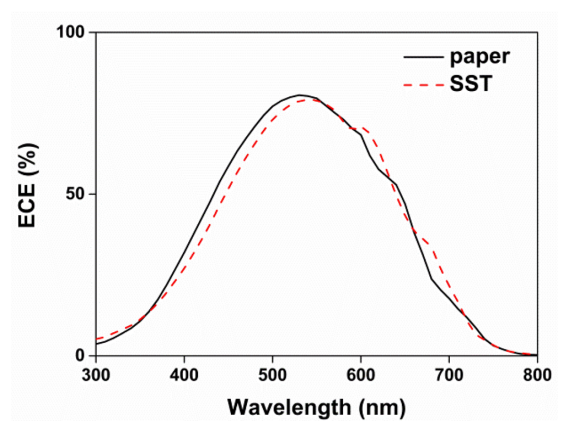


Figure 3 *J–V* curve (top) and ECE (bottom) of the best cell on paper and on stainless steel (SST).

anti-reflection properties, i.e. the thickness, of the ITO coating on top of the cells and has a small effect on the value of $J_{\rm SC}$.

The fill factor (FF), although fairly low, is systematically higher for the cells on stainless steel. This seems to be mainly caused by the lower $V_{\rm OC}$ and the somewhat higher "shunt resistance" (R_p) for these cells rather than by a reduced "series resistance". The slope of the J-V curve at 0 V and $V_{\rm OC}$ was taken to calculate $R_{\rm p}$ and $R_{\rm s}$, respectively. A more advanced method to derive these resistances uses an improved equivalent circuit and analytical model for a-Si: H solar cells, as proposed by Mertens et al. [13], but in the present cells the trends in R_p and R_s do not deviate from those in the resistances determined from the mathematical slopes. It is not completely clear what causes the difference in shunt resistance. In Fig. 4 a histogram of the R_p of all cells is shown. The rejection rate is comparable for both substrates showing it is not likely to be caused by the substrate itself but rather by the cell processing. The rejection rate is fairly high though. For (mini) module fabrication further effort should be put in optimizing the process with regards to the yield.

For the working cells the difference in R_p can be correlated to the substrates. On stainless steel the most frequent value of R_p is between 450 Ω cm² and 500 Ω cm² with the broadest tail to higher values (up to 700 Ω cm²) whereas



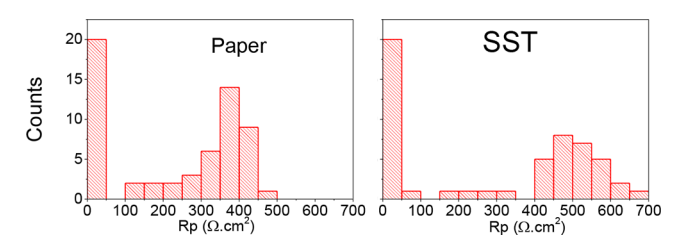


Figure 4 Histogram of the measured R_p values of all the cells on the paper (left) and stainless steel (right) substrate.

on paper the most frequent value lies between 350 Ω cm² and 400 Ω cm² with the broadest tail towards lower values. One can speculate that the cause lies in the lacquer, either the degassing or thermal deformation during the cell processing. Although on stainless steel also a lacquer layer is used this layer is about a factor 7 thinner than the total lacquer thickness of the paper substrate (~20 µm on SST vs. \sim 150 µm on paper). More importantly this layer is on one side encapsulated by the stainless steel substrate and on the other side (after the initial annealing/degassing step) with the Ag/ZnO: Al stack before it is exposed to elevated process temperatures. This encapsulation prevents eventual further degassing of the lacquer. In the case of paper the lacquer is only encapsulated on one side by the Ag/ZnO:Al stack. The total lacquer is so thick (~150 µm) that during the initial annealing/degassing the paper/lacquer bulk might not have been completely degassed. (Mind that the degassing rate of the lacquer was determined on a 20 µm thick layer.) The degassing may then proceed from the back side during further processing of the substrate at elevated temperatures and may introduce impurities in the subsequent layers, reducing the R_p . If the lacquer was not cured completely because of the single side exposure to UV light the degassing might be even more considerable. Part of the shunting behaviour can probably be improved by optimizing the curing and annealing process. In addition one could think of using different lacquers for the impregnation/planarization step and for the nano-imprinting step.

4 Conclusion Commodity printing paper, which has a very open structure consisting of fibres, can be planarized by impregnating it with an UV curable acrylate lacquer. The surface can then be nano-textured by applying a second, thinner, layer of the same lacquer that is imprinted and cured. Due to the softness of the substrate the morphology of the imprinted texture differs slightly from that on a stainless steel substrate.

The overall performance of HWCVD a-Si:H solar cells on paper and stainless steel substrates is comparable although the $V_{\rm OC}$ is significantly (90 mV) higher for cells on paper, whereas the shunt resistance and thus the fill factor is better for the cells on stainless steel. The cause of the

lower shunt resistance might be found in the degassing of the lacquer. Further optimization of the planarization and imprinting process can lead to even better performance and higher yield. In conclusion, a procedure is present due to which commodity paper is a suitable candidate to act as a substrate for a-Si:H solar cells and (mini) modules without making any concessions to the a-Si:H process temperature of 200 °C. The efficiency reached is now comparable to the typical efficiency obtained for a-Si:H cells on more common substrates such as stainless steel, paving the way towards novel applications on commodity paper like newspaper paper or even fabric.

Acknowledgements This work was partially funded by the Dutch Ministry of Economic affairs in the framework of the TKI Project LIMANIL (TKIZ01010). The authors thank Utrecht University for the use of their cluster tool.

References

- [1] R. E. I. Schropp, Thin Solid Films, DOI: 10.1016/j.tsf.2015.07.054 (2015).
- [2] A. Franken, H. Li, R. Stolk, K. van der Werf, J. Rath, and R. Schropp, Stable, high deposition rate, wide gap silicon for the rather thick top cells in thin film silicon multibandgap solar cells, 4th World Conference on Photovoltaic Energy Conversion, 2006, pp. 1497–1499, DOI: 10.1109/WCPEC.2006.279753 (2006).
- [3] B. Wang and L. L. Kerr, Sol. Energy Mater. Sol. Cells 95, 2531–2535 (2011).
- [4] Z. Fang, H. Zhu, Y. Yuan, D. Ha, S. Zhu, C. Preston, Q. Chen, Y. Li, X. Han, S. Lee, G. Chen, T. Li, J. Munday, J. Huang, and L. Hu, Novel Nano Lett. 14, 765–773 (2014).
- [5] Y. Zhou, C. Fuentes-Hernandez, T. M. Khan, J.-C. Liu, J. Hsu, J. W. Shim, A. Dindar, J. P. Youngblood, R. J. Moon, and B. Kippelen, Sci. Rep. 3, 1536 (2013).
- [6] H. Aguas, T. Mateus, A. Vicente, D. Gaspar, M. J. Mendes, W. A. Schmidt, L. Pereira, E. Fortunato, and R. Martins, Adv. Funct. Mater. 25, 3592–3598 (2015).
- [7] B. B. Van Aken, J. Löffler, M. C. R. Heijna, and W. J. Soppe, J. Non-Cryst. Solids 358, 2268–2271 (2012).
- [8] W. Soppe, M. Dörenkämper, J.-B. Notta, P. Pex, W. Schipper, and R. Wilde, Phys. Status Solidi A 210, 707–710 (2013).
- [9] R. E. I. Schropp, K. F. Feenstra, E. C. Molenbroek, H. Meiling, J. K. Rath, Philos. Mag. B 76, 309–321 (1997).
- [10] T. Söderström, F.-J. Haug, V. Terrazzoni-Daudrix, and C. Ballif, J. Appl. Phys. **103**, 114509 (2008).
- [11] M. Python, E. Vallat-Sauvain, J. Bailat, D. Dominé, L. Fesquet, A. Shah, and C. Ballif, J. Non-Cryst. Solids 354, 2258–2262 (2008).
- [12] H. B.T. Li, R. H. Franken, J. K. Rath, and R. E. I. Schropp, Solar Energy Mater. Sol. Cells 93, 338–349 (2009).
- [13] J. Merten, J. M. Asensi, C. Voz, A. V. Shah, R. Platz, and J. IEEE Trans. Electron Devices 45, 423–429 (1998).